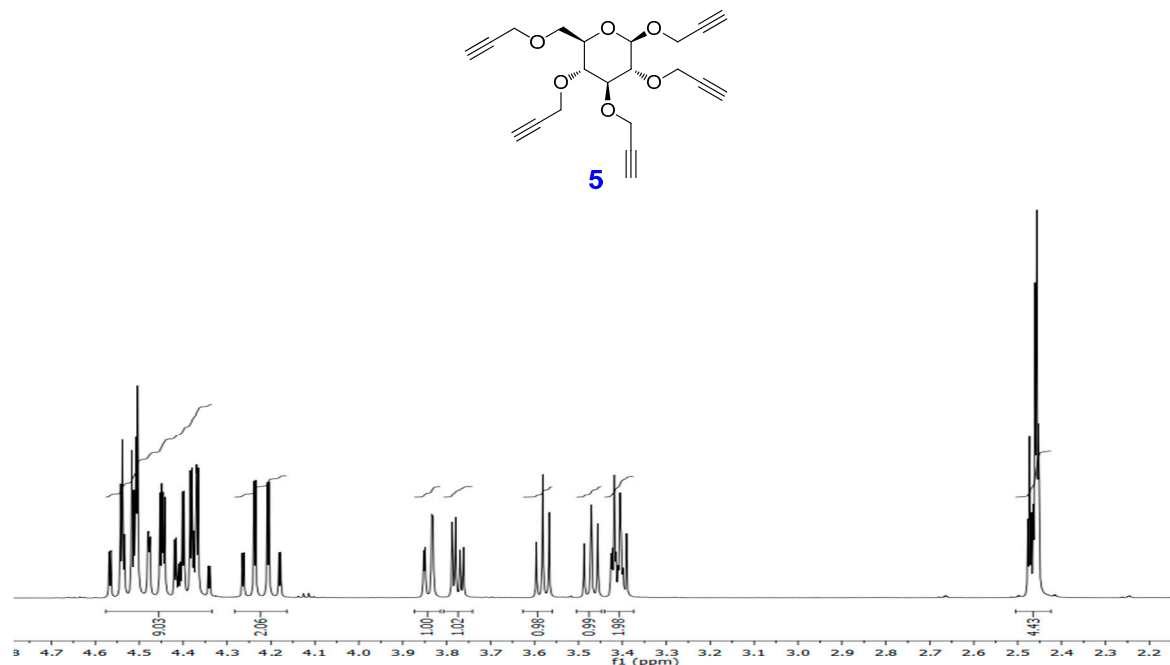


# Supplementary Information: Synthesis of Dense and Chiral Dendritic Polyols Using Glyconanosynthon Scaffolds

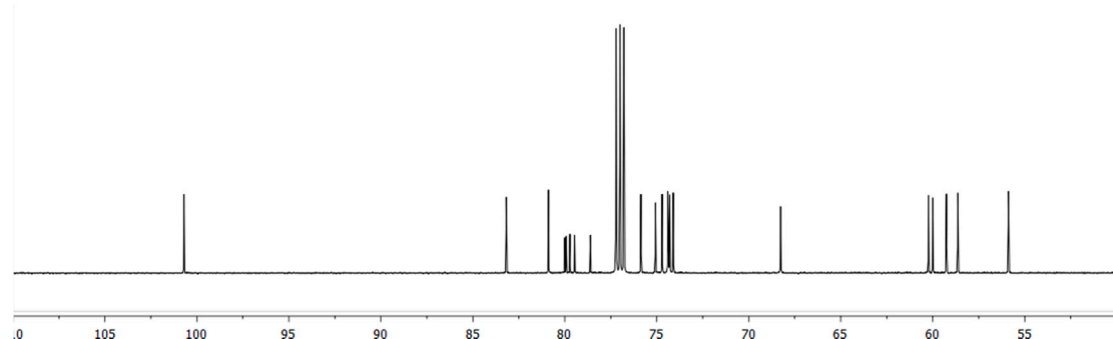
Tze Chieh Shiao, Rabindra Rej, Mariecka Rose, Giovanni M. Pavan and René Roy

## 1. Characterizations ( $^1\text{H}$ , $^{13}\text{C}$ and COSY NMR; HRMS and GPC)

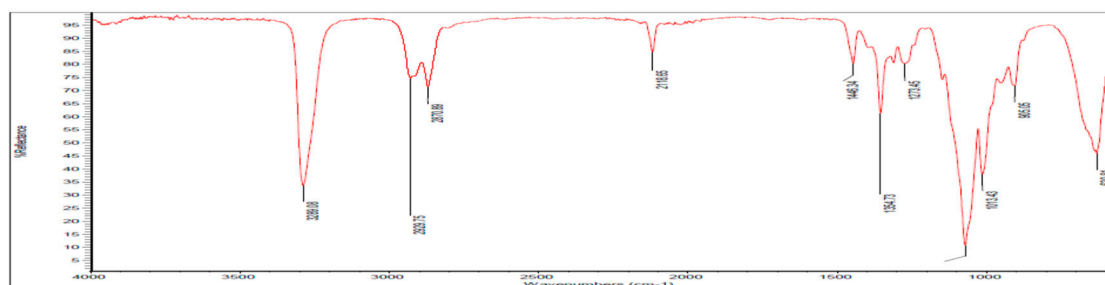
### 1.1. Propargyl 2,3,4,6-tetra-O-propargyl- $\beta$ -D-glucopyranoside (5)



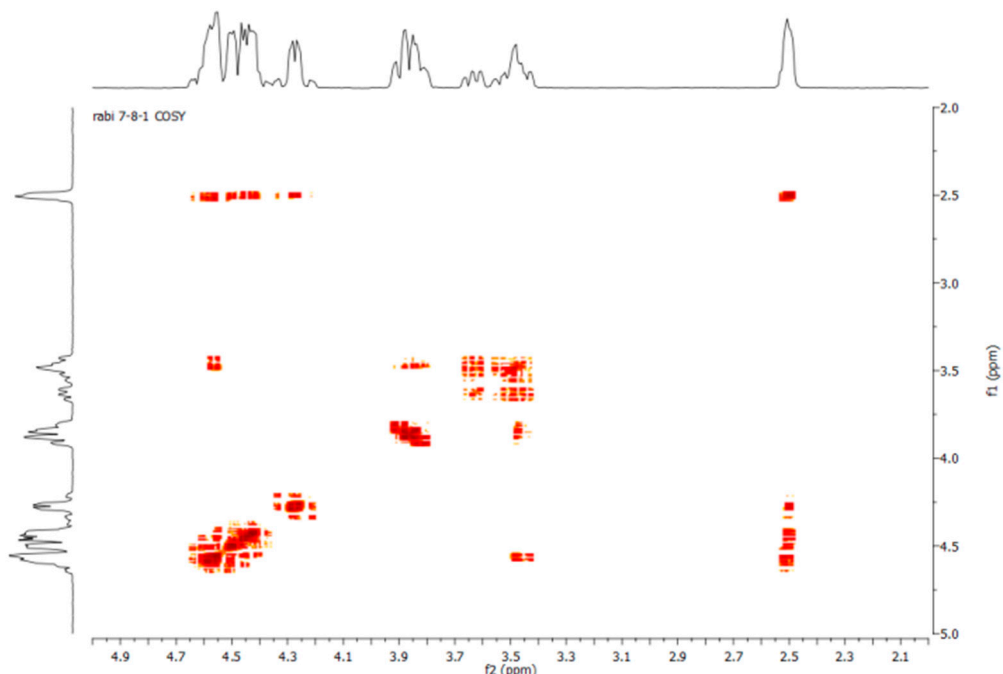
**Figure S1.**  $^1\text{H}$ -NMR spectrum of Propargyl 2,3,4,6-tetra-O-propargyl- $\beta$ -D-glucopyranoside (5).



**Figure S2.**  $^{13}\text{C}$ -NMR spectrum of Propargyl 2,3,4,6-tetra-O-propargyl- $\beta$ -D-glucopyranoside (5).

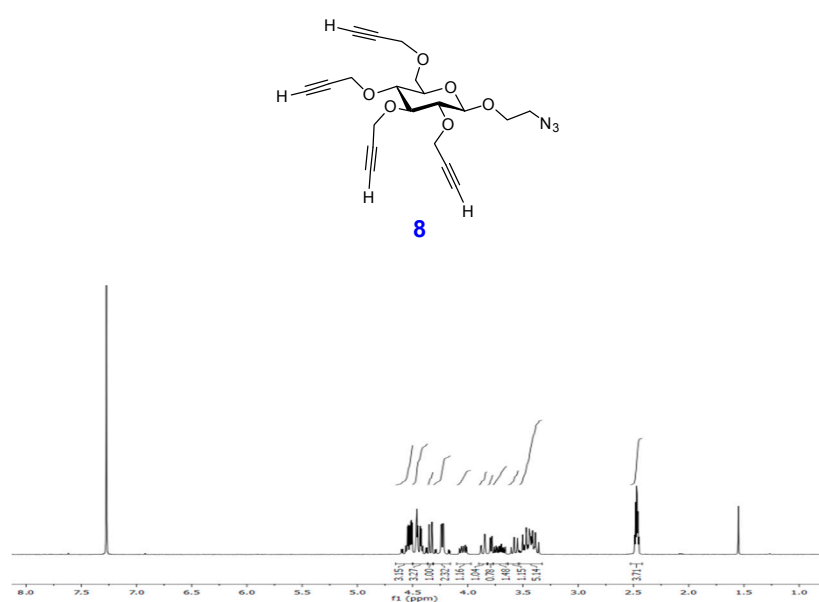


**Figure S3.** IR spectrum of Propargyl 2,3,4,6-tetra-O-propargyl- $\beta$ -D-glucopyranoside (**5**).

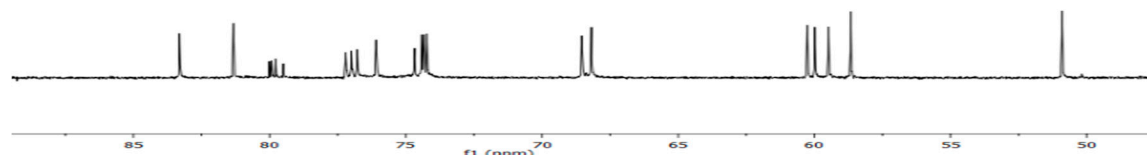


**Figure S4.** <sup>1</sup>H-<sup>1</sup>H COSY-NMR of **5**.

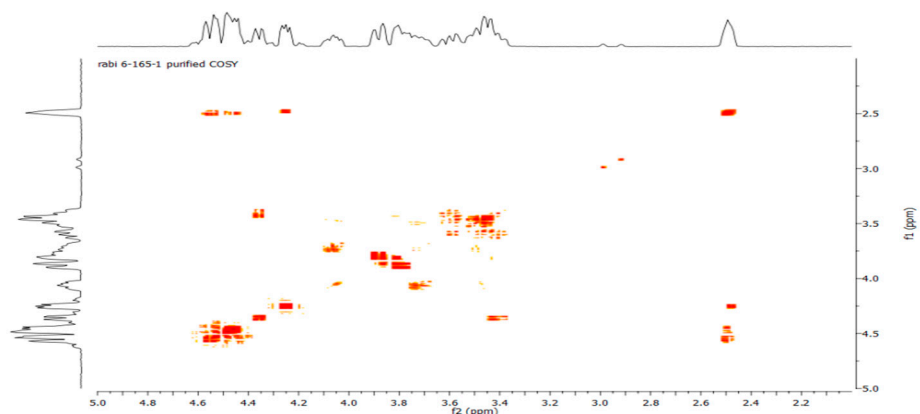
#### 1.2. 2-Azidoethyl 2,3,4,6-tetra-O-propargyl- $\beta$ -D-glucopyranoside (**8**)



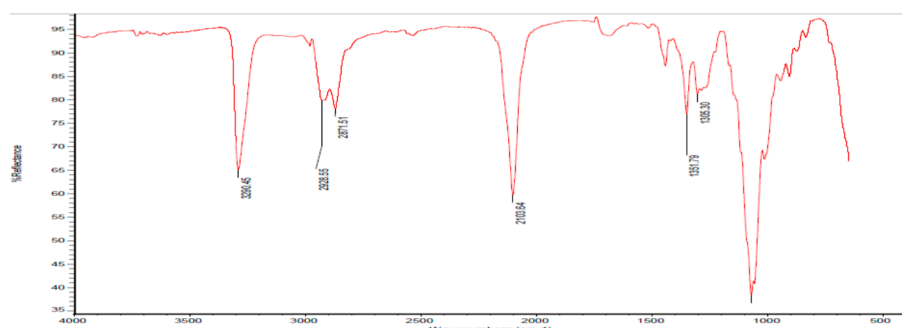
**Figure S5.** <sup>1</sup>H-NMR spectrum of 2-azidoethyl 2,3,4,6-tetra-O-propargyl- $\beta$ -D-glucopyranoside (**8**).



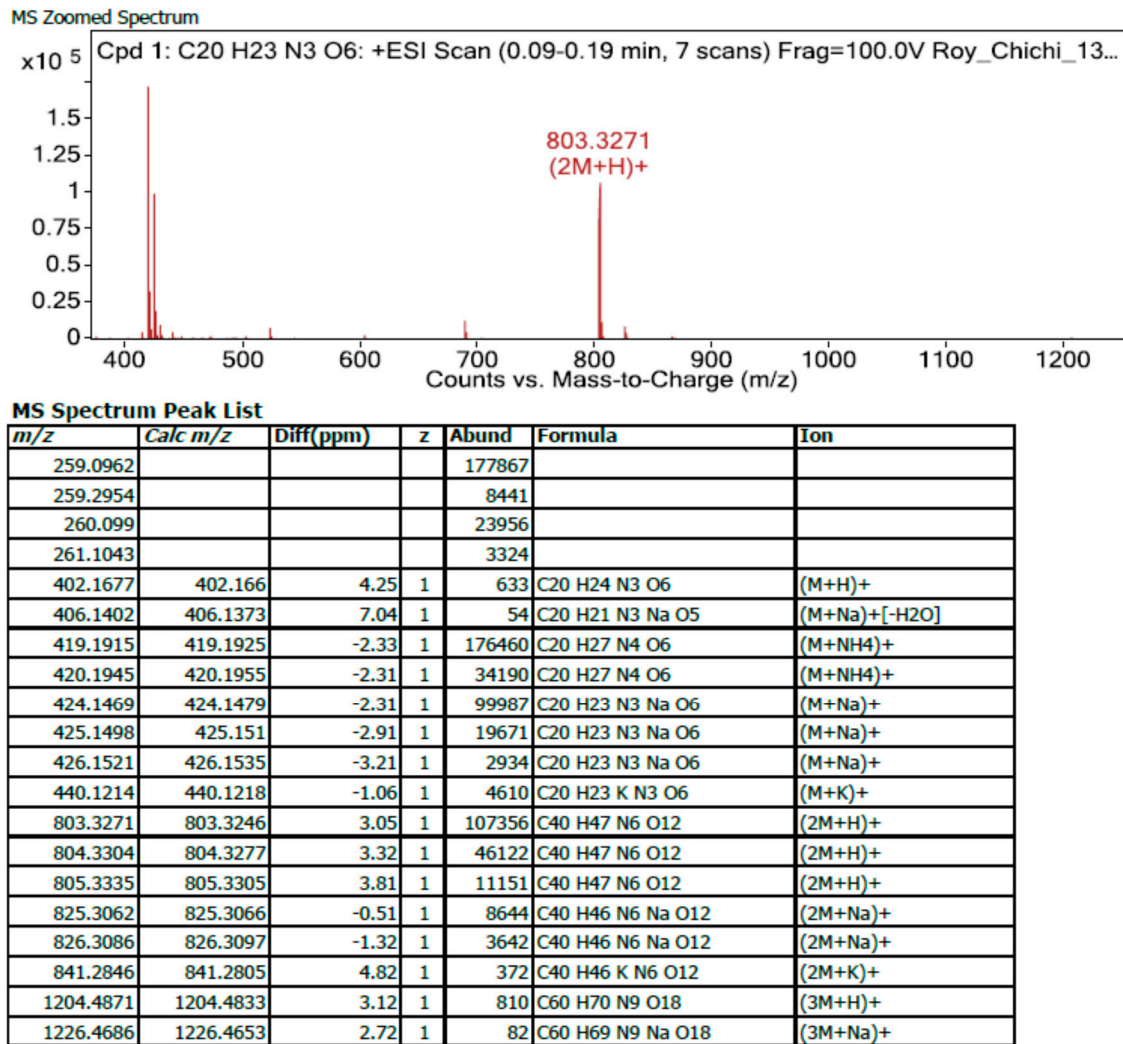
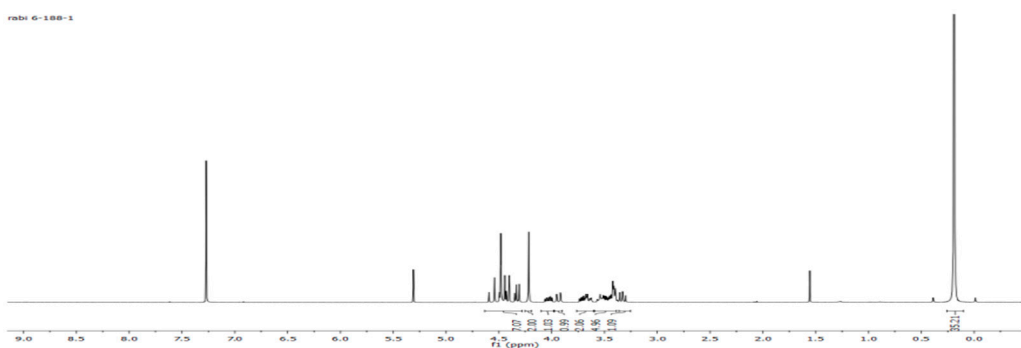
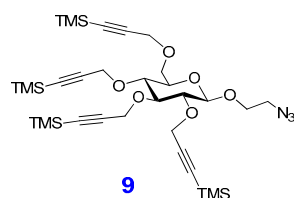
**Figure S6.** <sup>13</sup>C-NMR spectrum of 2-azidoethyl 2,3,4,6-tetra-O-propargyl- $\beta$ -D-glucopyranoside (8).



**Figure S7.** <sup>1</sup>H-<sup>1</sup>H COSY-NMR of 2-azidoethyl 2,3,4,6-tetra-O-propargyl- $\beta$ -D-glucopyranoside (8).



**Figure S8.** IR spectrum of 8.

**Figure S9.** High resolution mass spectrum of 8.**1.3. 2-Azidoethyl 2,3,4,6-tetra-O-trimethylsilylpropargyl- $\beta$ -D-glucopyranoside (9)****Figure S10.** <sup>1</sup>H-NMR spectrum of 9.

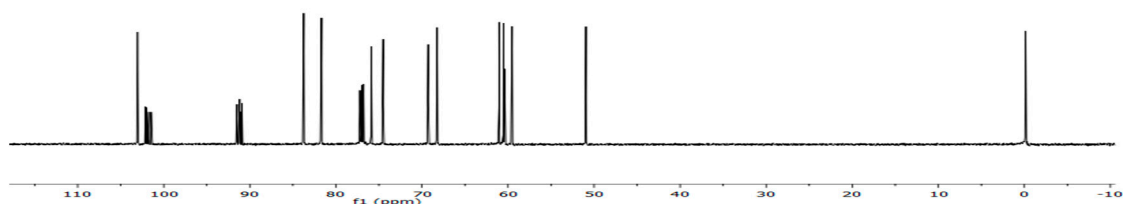


Figure S11.  $^{13}\text{C}$ -NMR spectrum of 9.

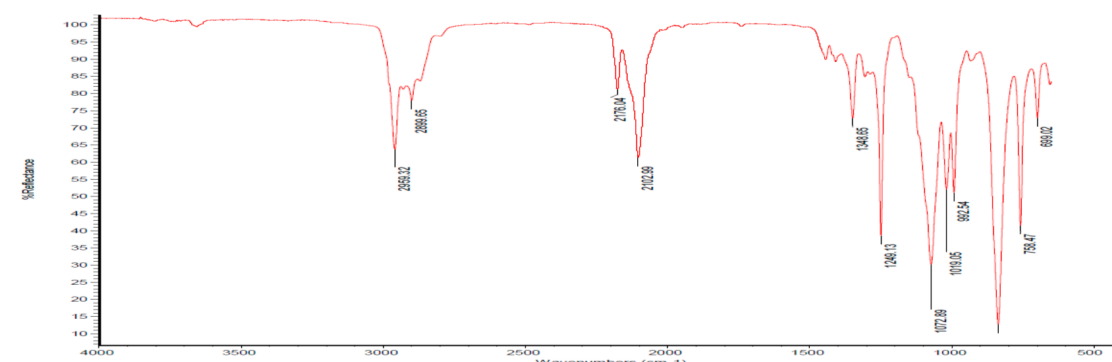


Figure S12. IR spectrum of 9.

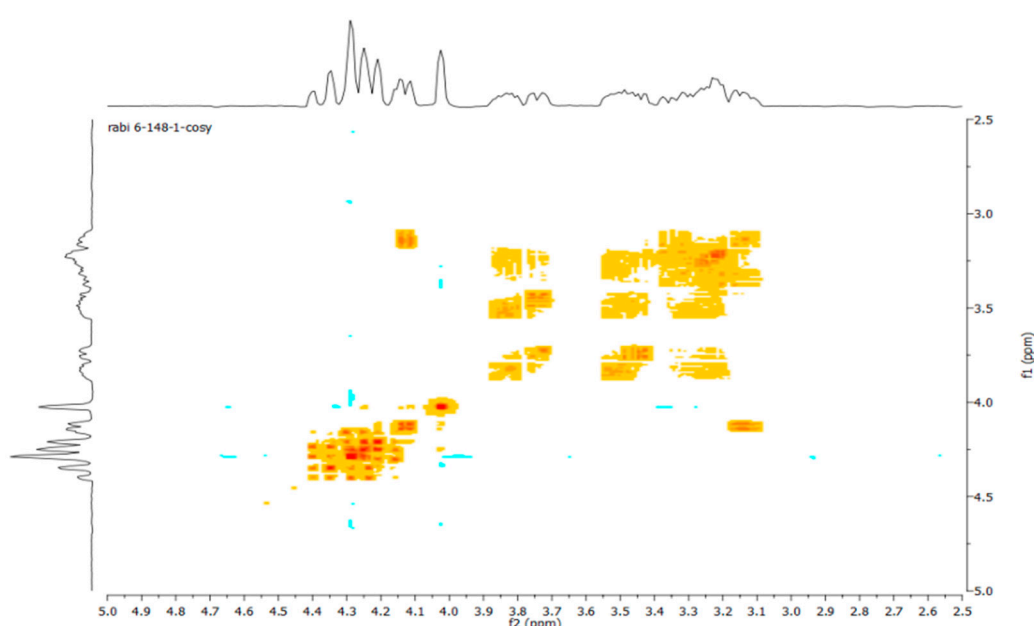


Figure S13.  $^1\text{H}$ - $^1\text{H}$  COSY-NMR of 9.

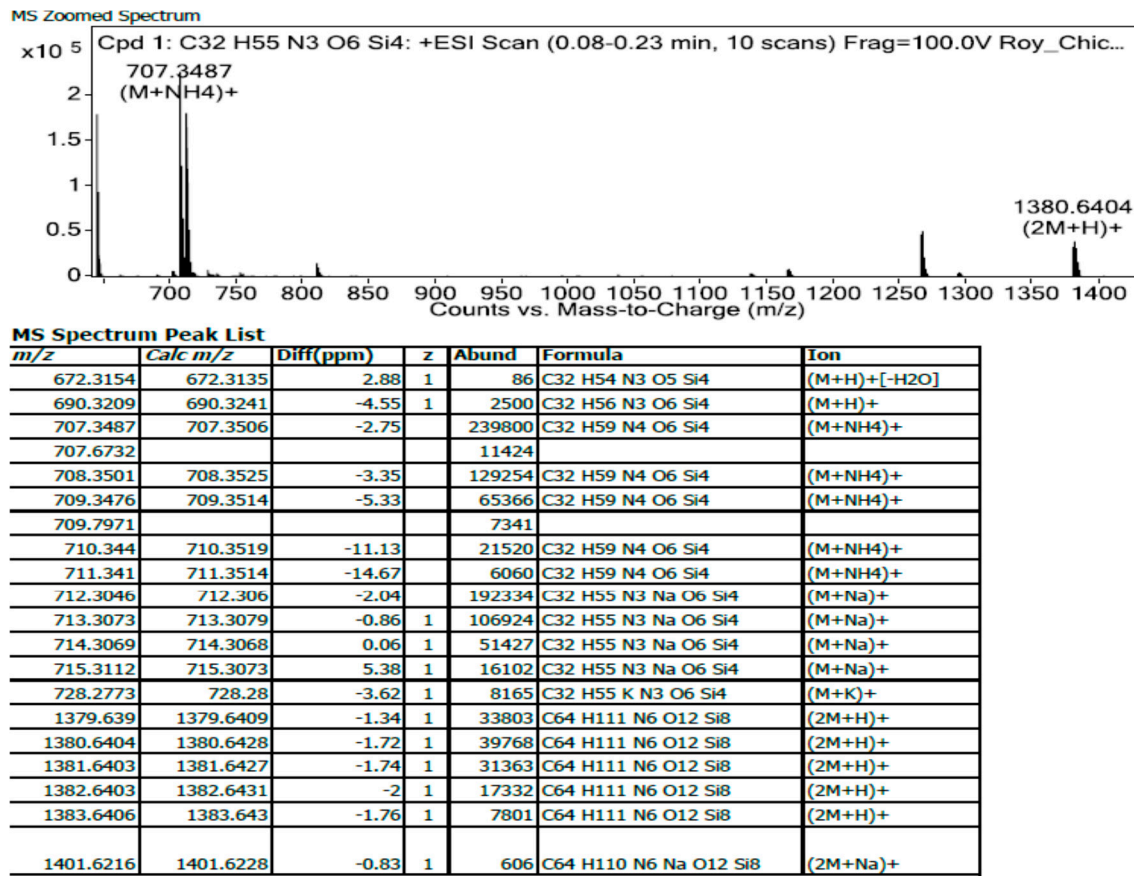
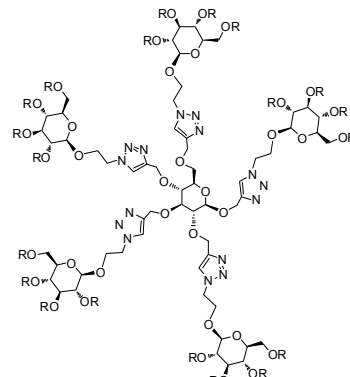
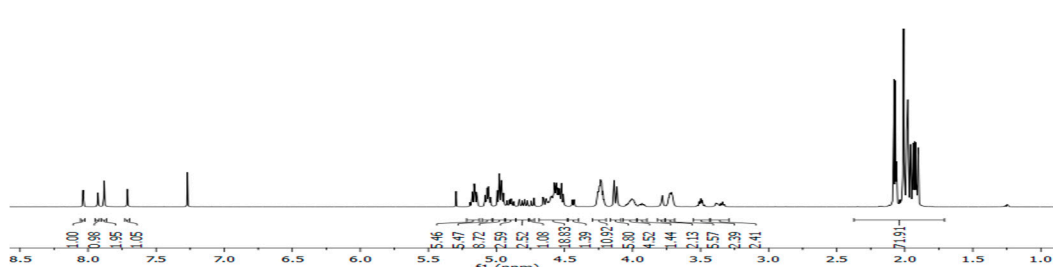


Figure S14. High resolution mass spectrum of 9.

#### 1.4. Dendrimer 10

**G<sub>1</sub> = 20-OAc**Figure S15. <sup>1</sup>H-NMR spectrum of 10.

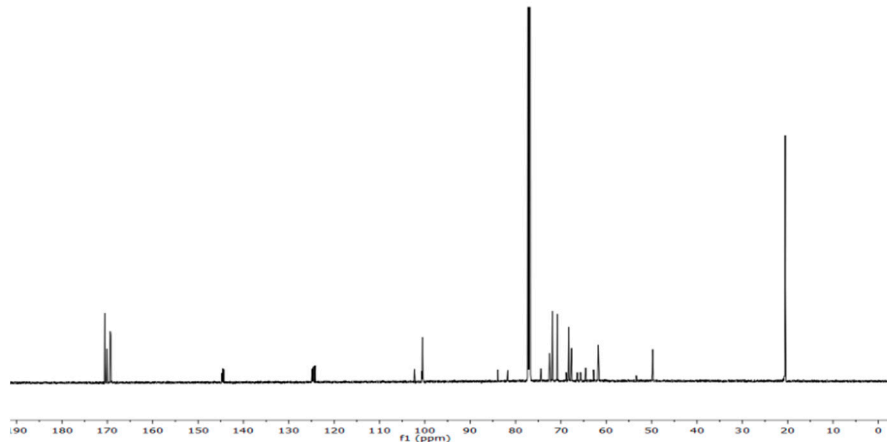
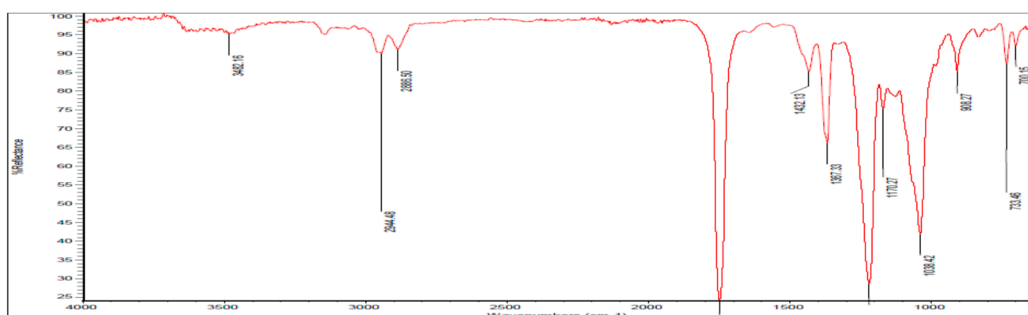
Figure S16.  $^{13}\text{C}$ -NMR spectrum of 10.

Figure S17. IR spectrum of 10.

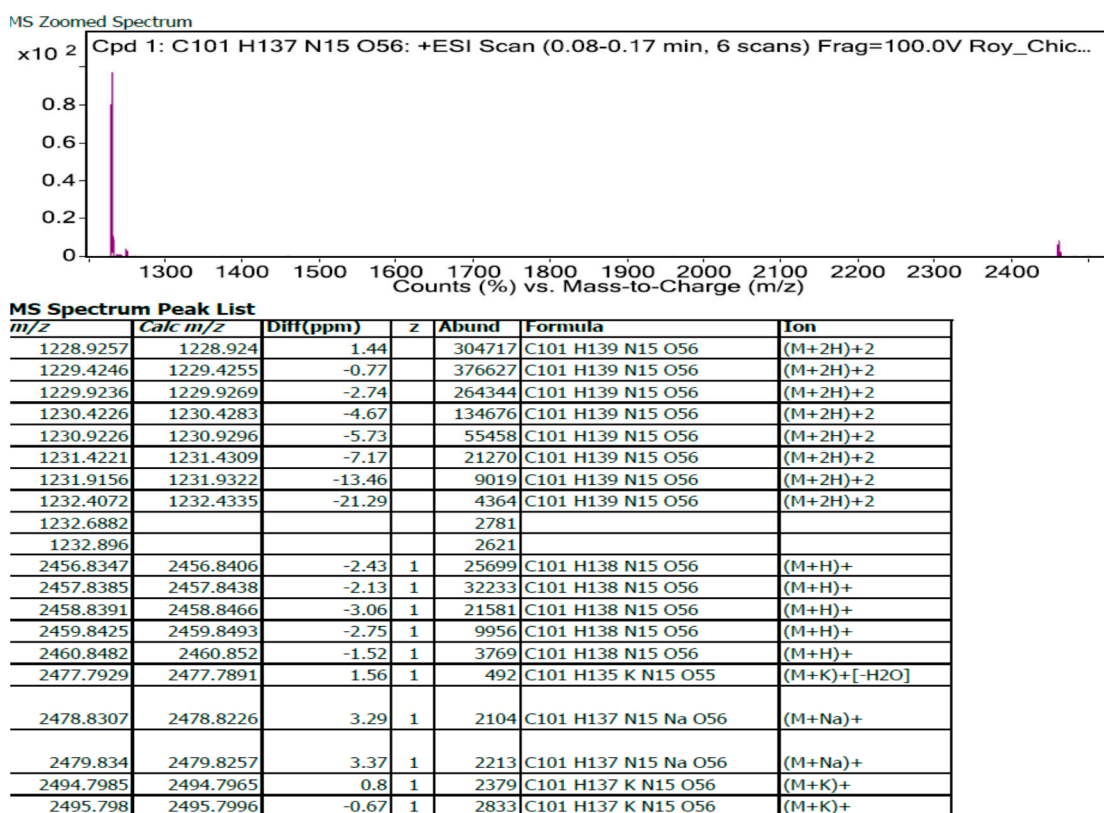
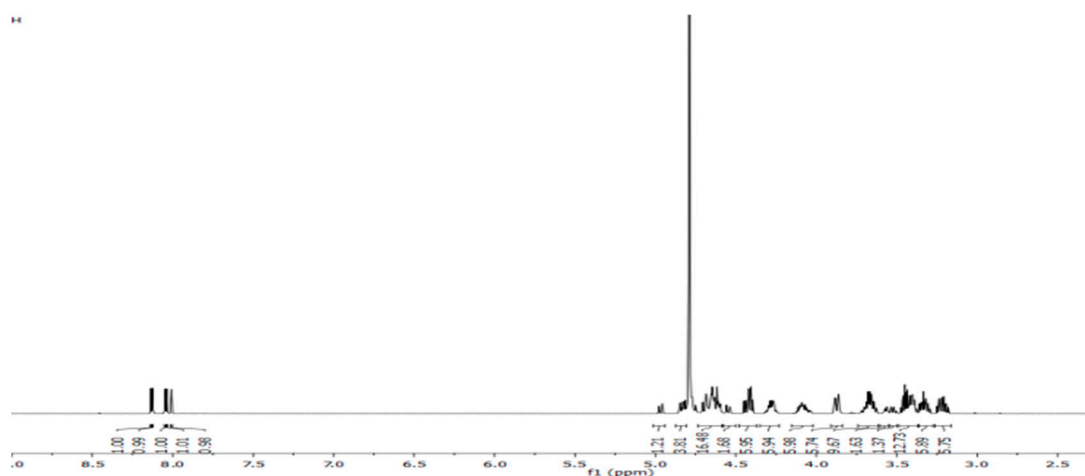
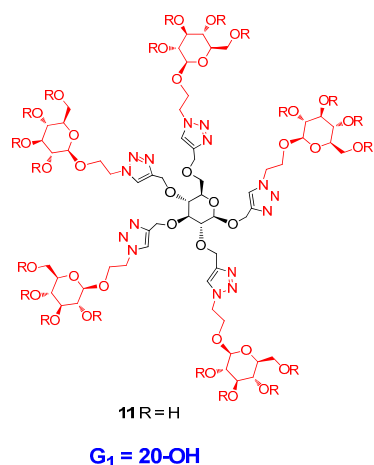
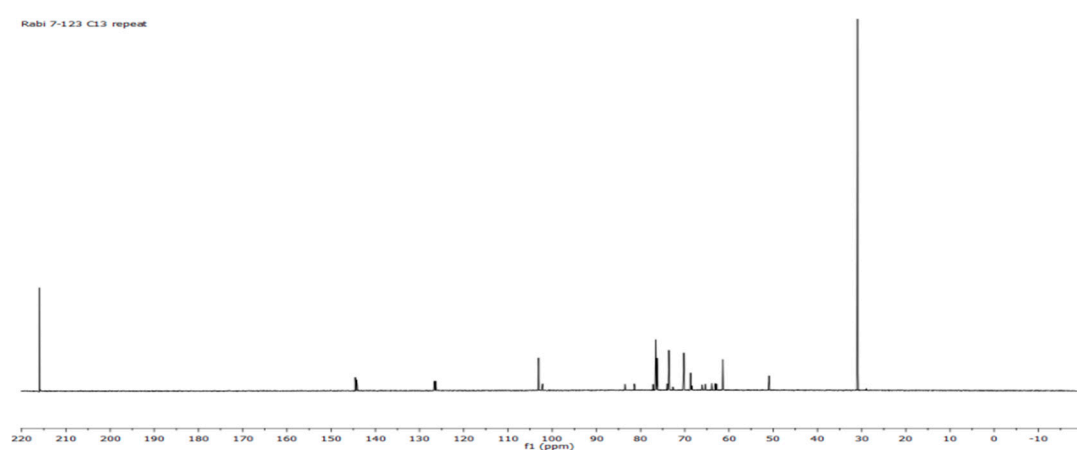


Figure S18. High resolution mass spectrum of (10).

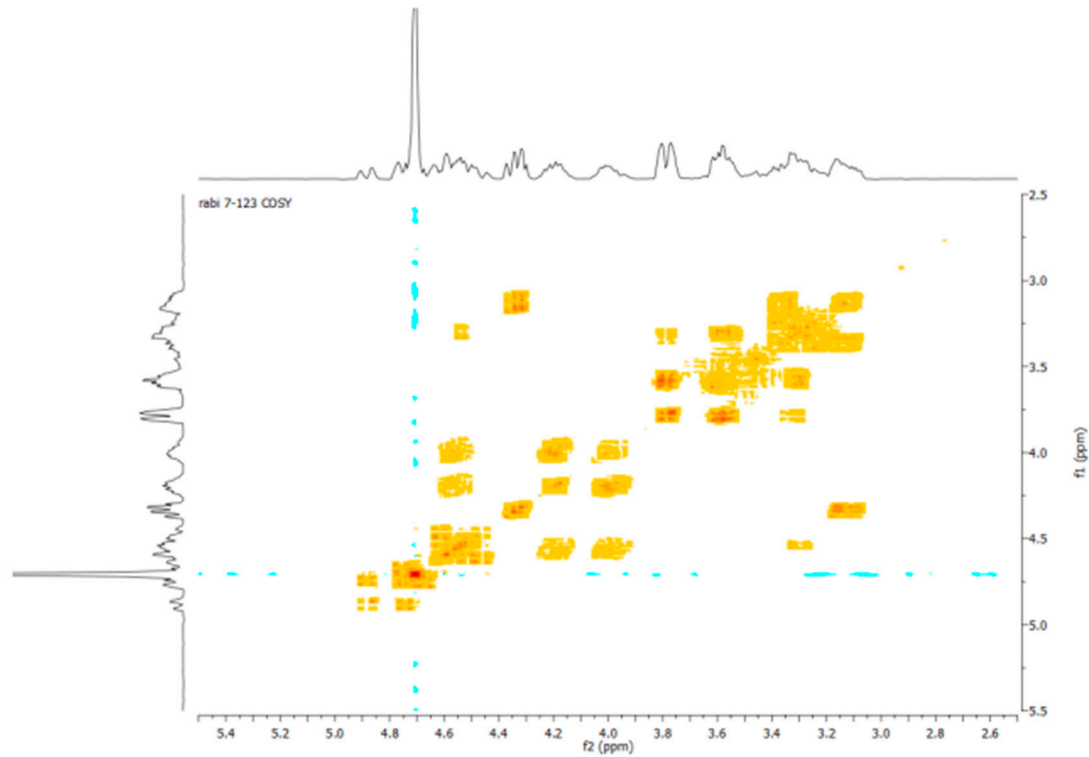
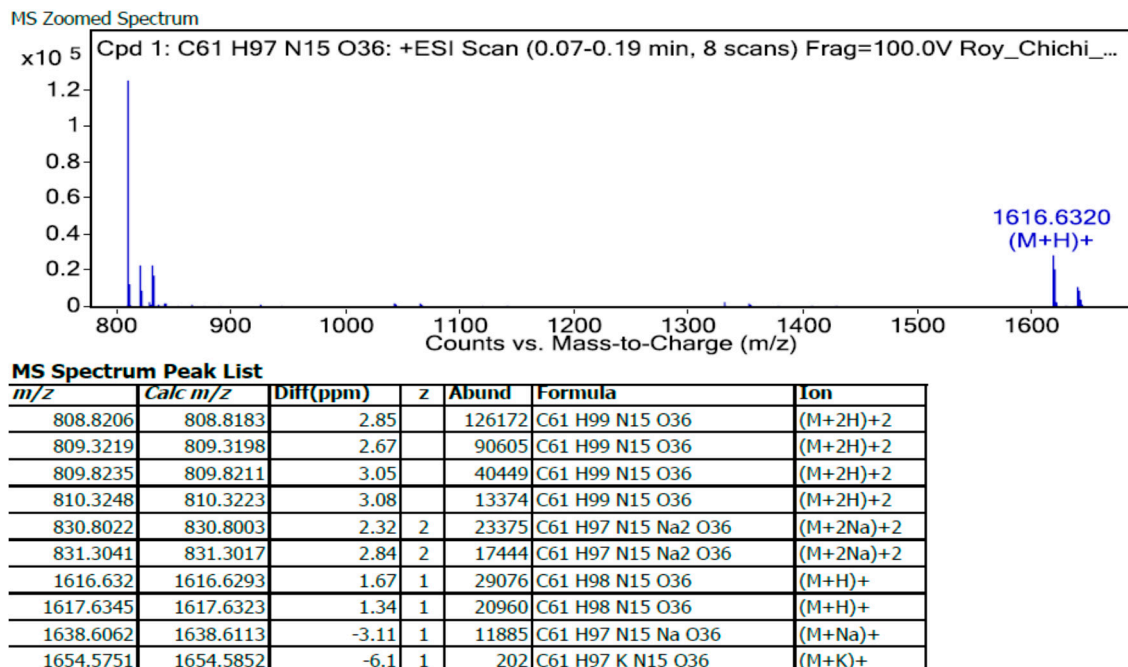
### 1.5. Dendrimer 11



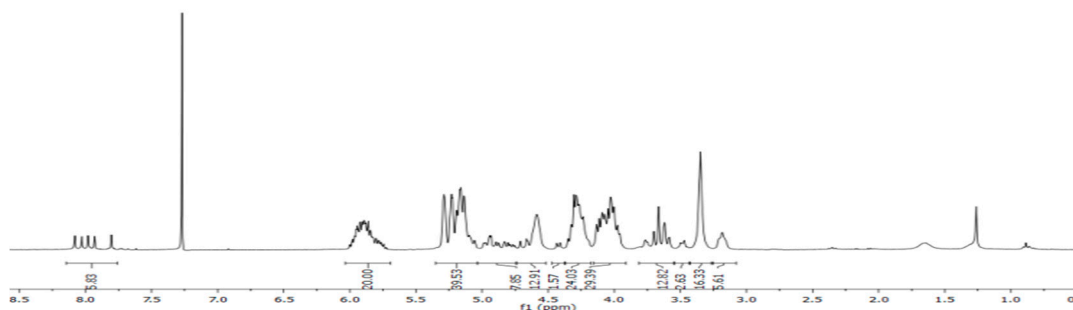
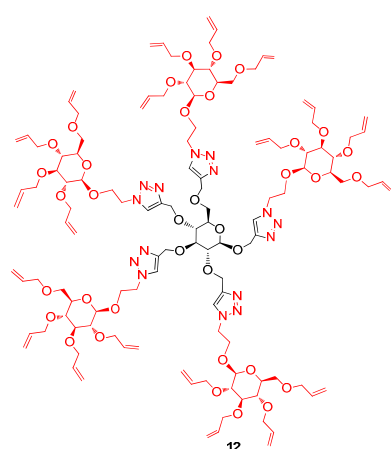
**Figure S19.**  $^1\text{H}$ -NMR spectrum of **11**.



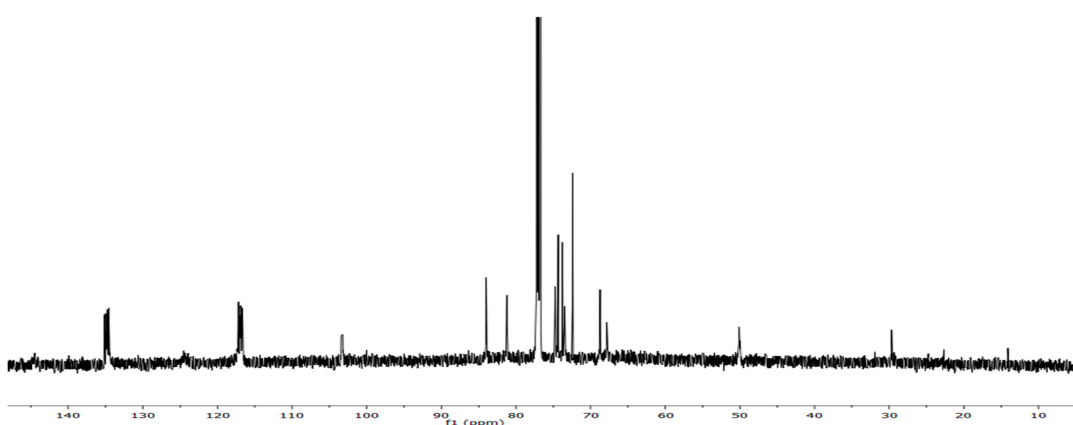
**Figure S20.**  $^{13}\text{C}$ -NMR spectrum of **11**.

Figure S21.  $^1\text{H}$ - $^1\text{H}$  COSY-NMR of **11**.Figure S22. High resolution mass spectrum of **11**.

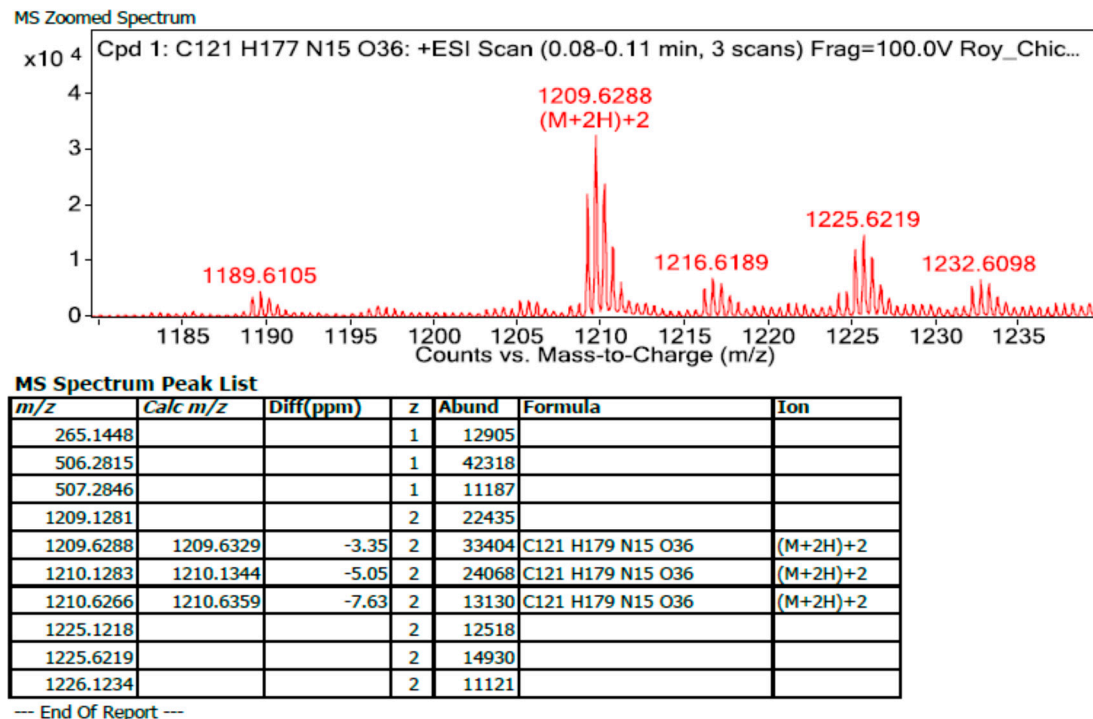
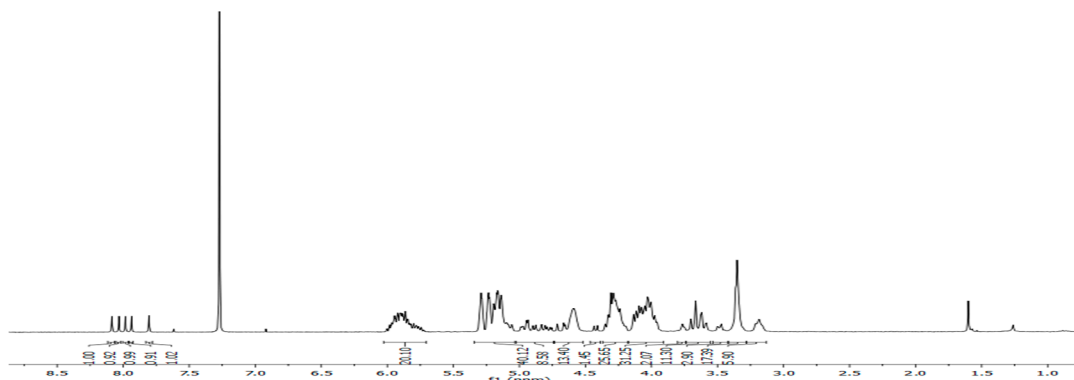
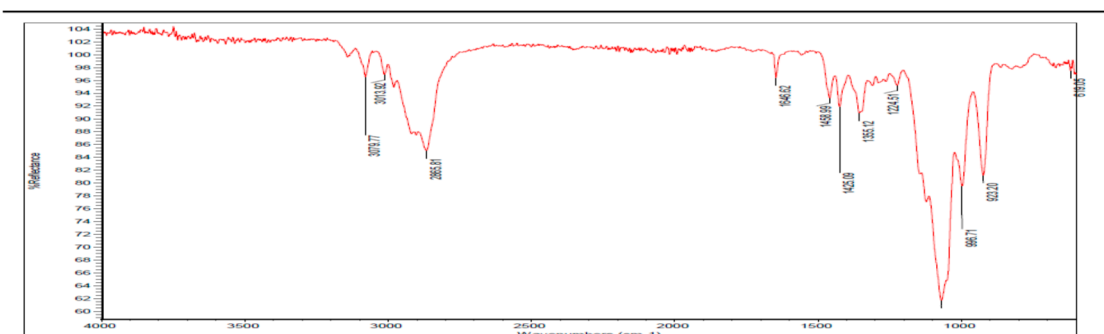
### 1.6. Dendrimer 12



**Figure S23.** <sup>1</sup>H-NMR spectrum of **12** obtained by direct allylation.



**Figure S24.** <sup>13</sup>C-NMR spectrum of **12**.

**Figure S25.** High resolution mass spectrum of **12**.**Figure S26.** <sup>1</sup>H-NMR spectrum of **12** obtained from Click reaction.**Figure S27.** IR spectrum of **12** obtained from Click reaction.

1.7. Dendrimer 13

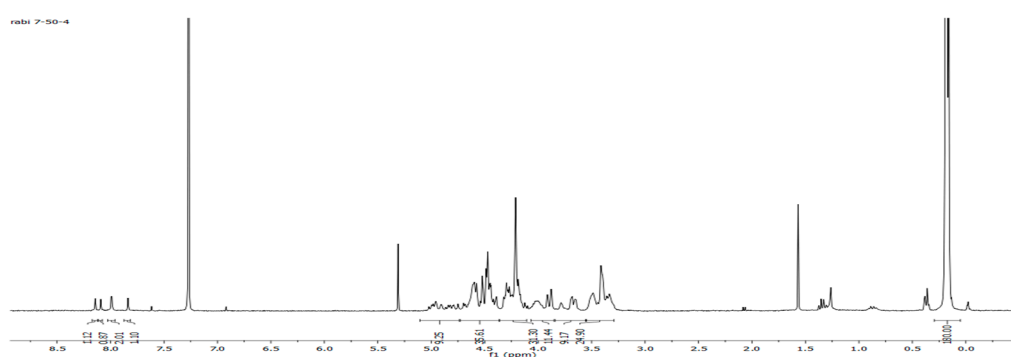
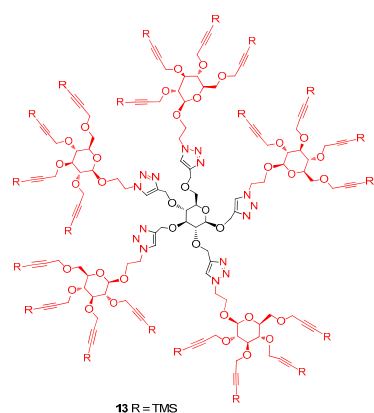


**Figure S28.**  $^1\text{H}$ -NMR( $\text{CDCl}_3$ ) of **13**.

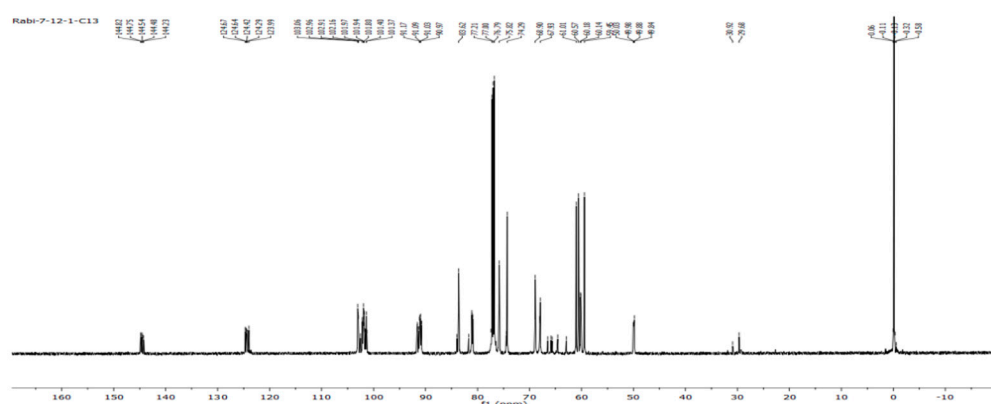


**Figure S29.**  $^{13}\text{C}$ -NMR spectrum of **13**.

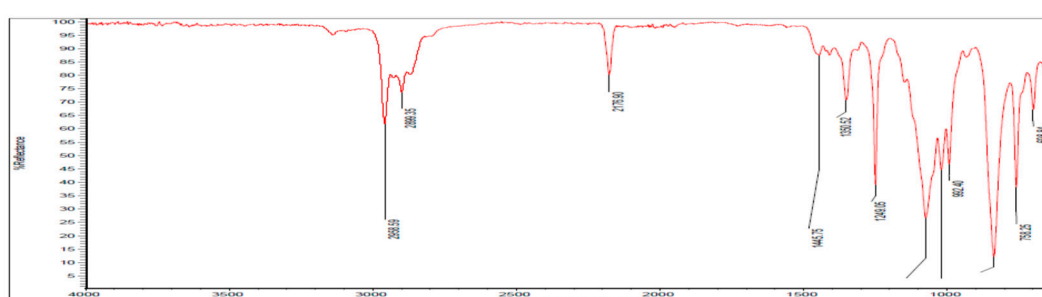


**Figure S30.** IR spectrum of 13.

### 1.8. Dendrimer 14

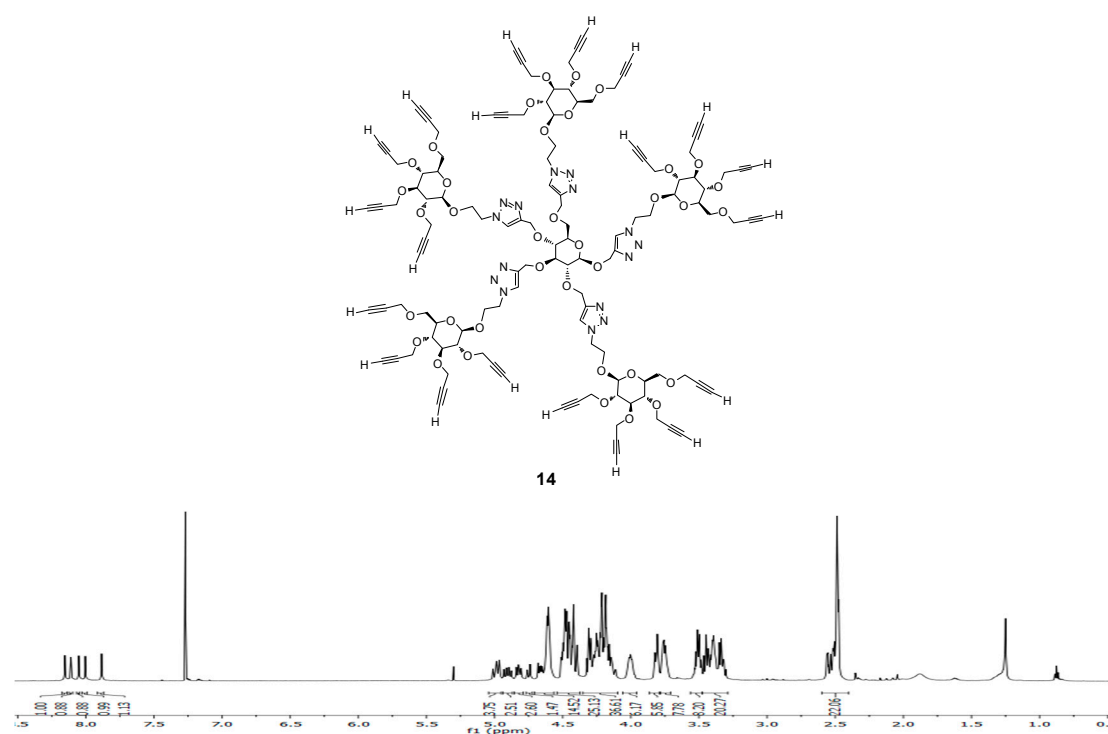


**Figure S31.** <sup>1</sup>H-NMR ( $\text{CDCl}_3$ ) spectrum of **14**.

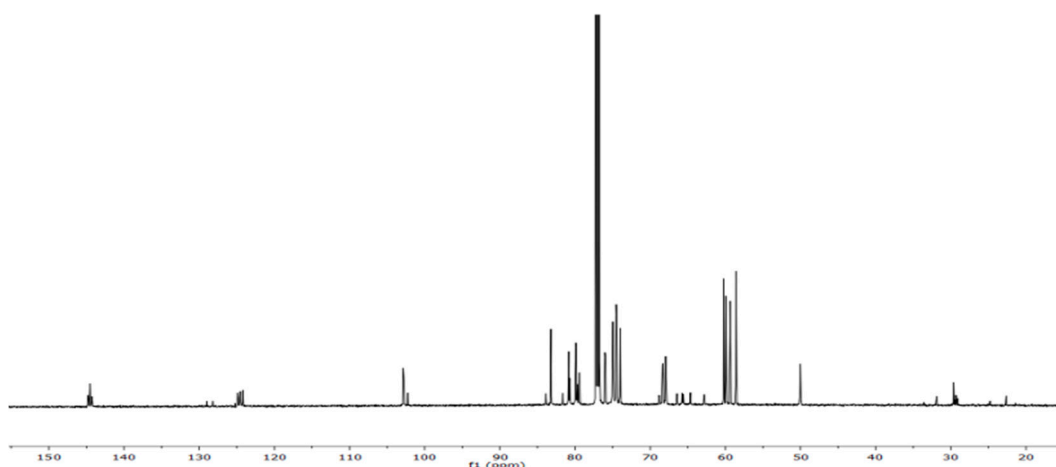


**Figure S32.** <sup>13</sup>C-NMR spectrum of **14**.

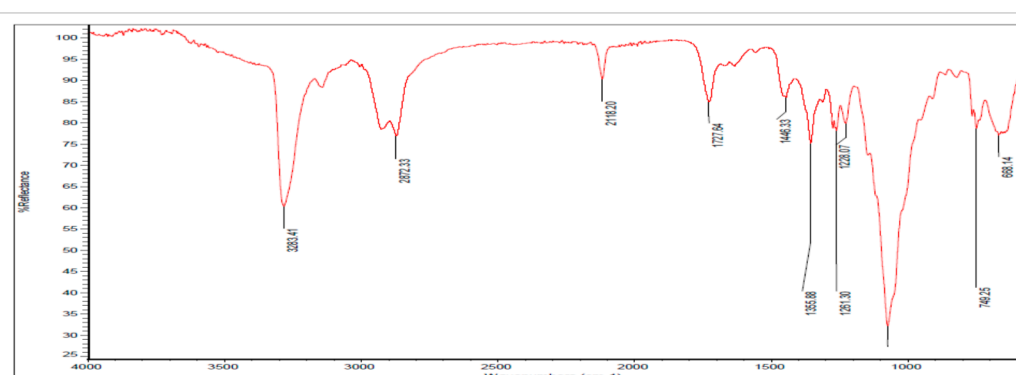


**Figure S33.** IR spectrum of **14**.

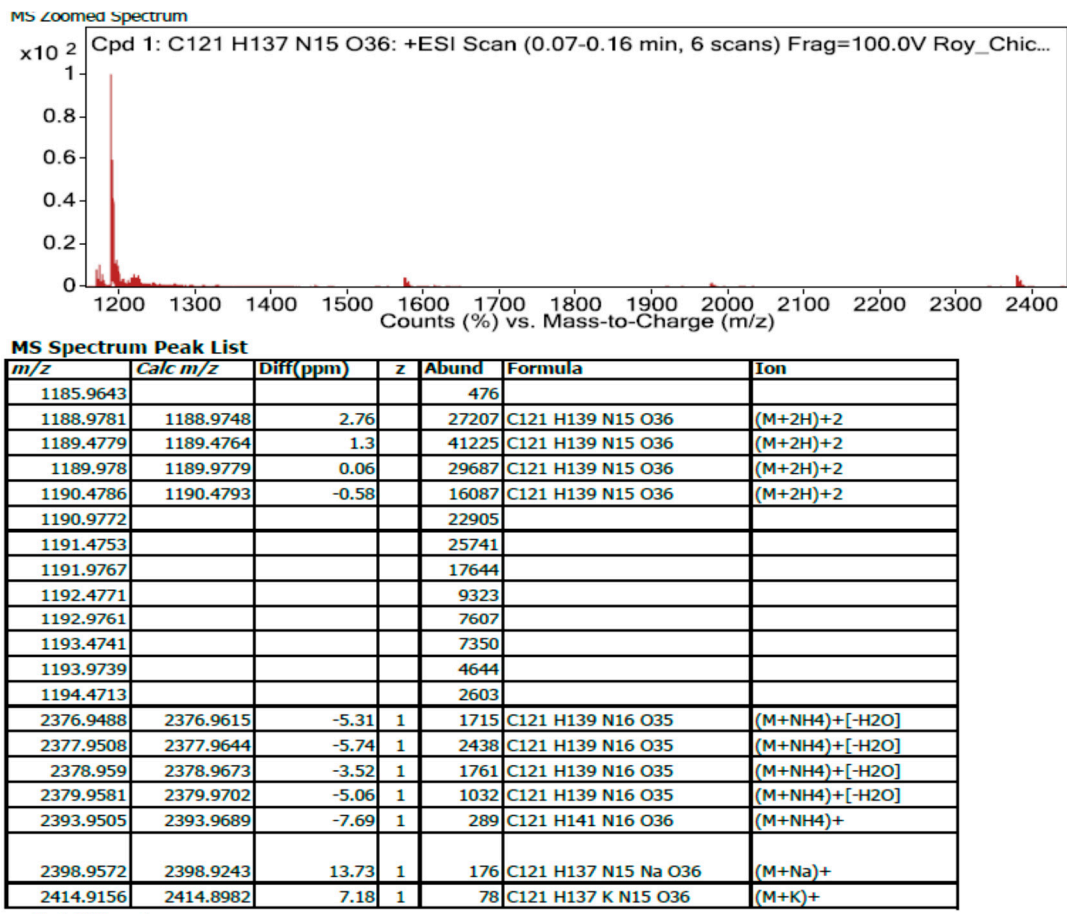
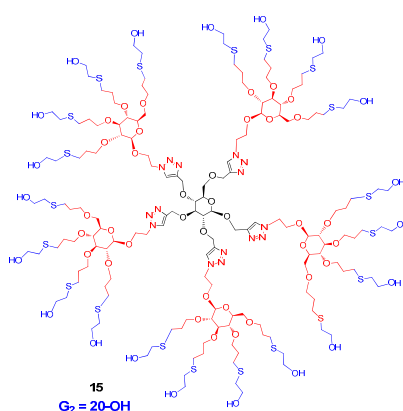
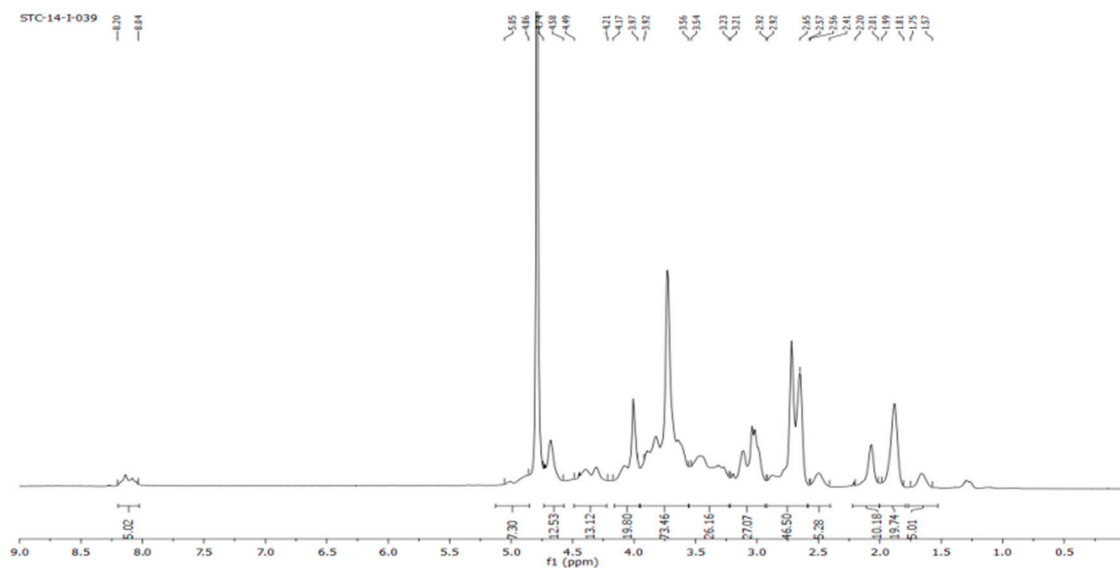


Figure S34. High resolution mass spectrum of 14.

### 1.9. Dendrimer 15





**Figure S35.**  $^1\text{H}$ -NMR ( $\text{D}_2\text{O}$ ) spectrum of **15**.

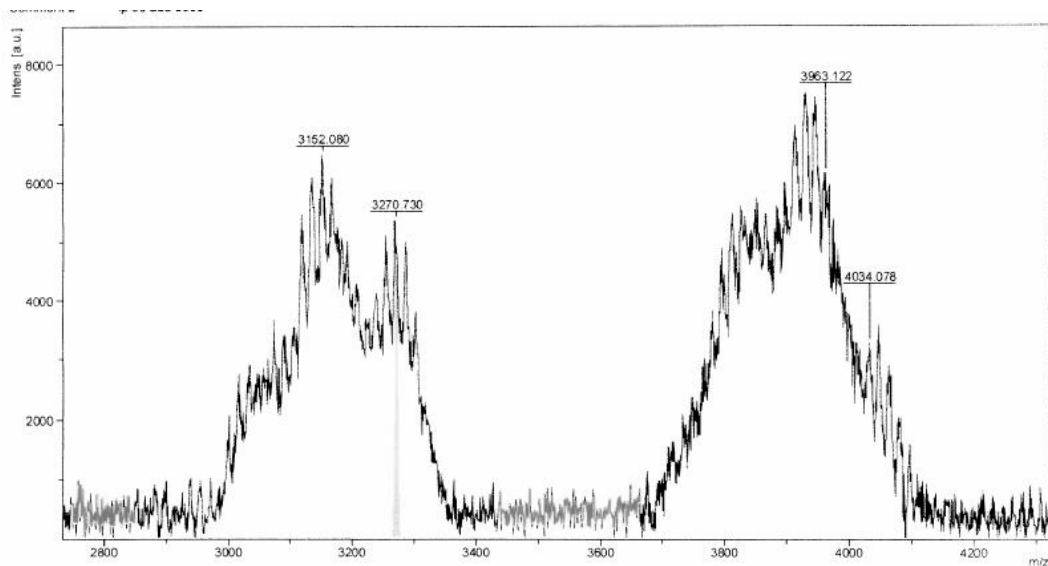


**Figure S36.** Maldi-tof of compound **15**.

### 1.10. Dendrimer 16

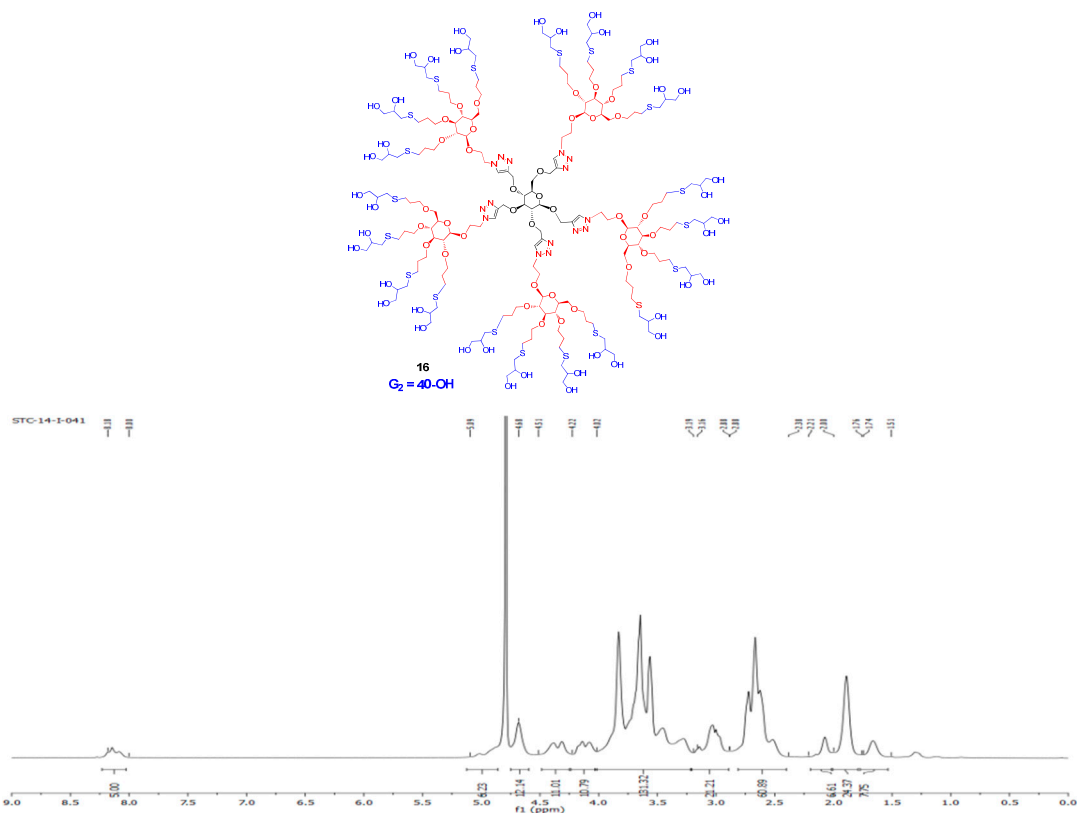


**Figure S37.** <sup>1</sup>H-NMR (D<sub>2</sub>O) spectrum of **16**.

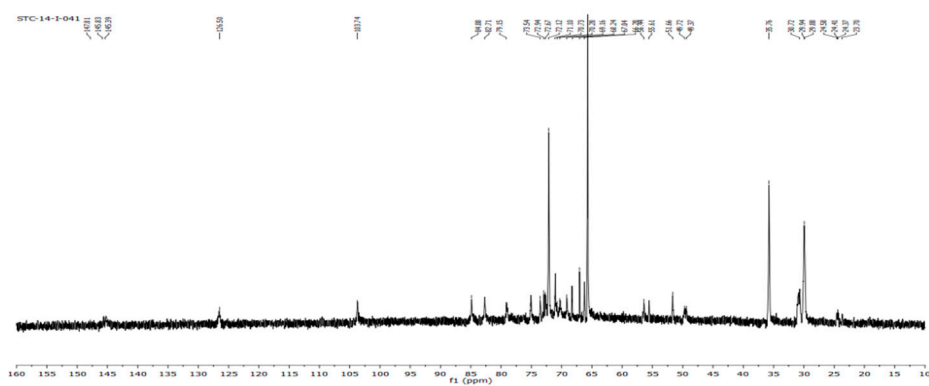


**Figure S38.** <sup>13</sup>C-NMR of **16**.

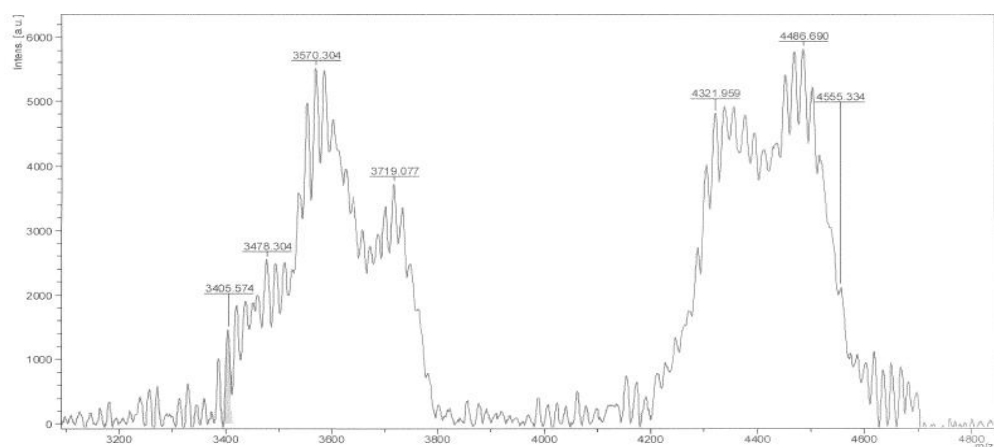


**Figure S39.** Maldi-tof of Compound **16**.

### 1.11. Dendrimer **17**

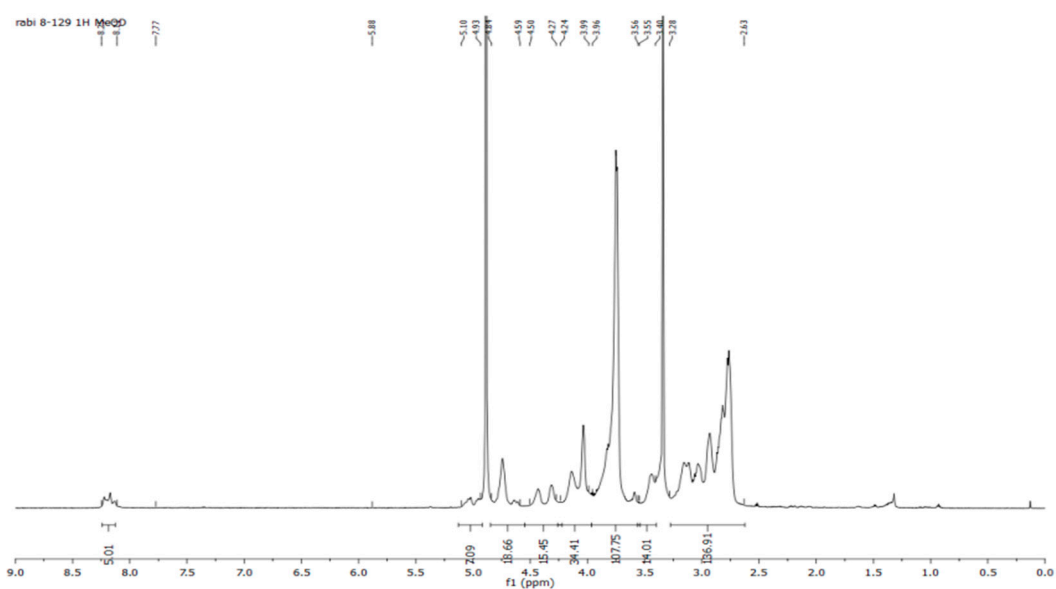
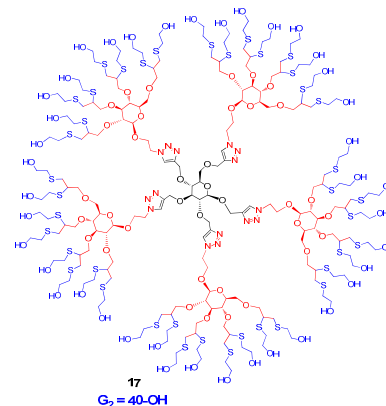


**Figure S40.** <sup>1</sup>H-NMR ( $\text{D}_2\text{O}$ ) spectrum of **17**.

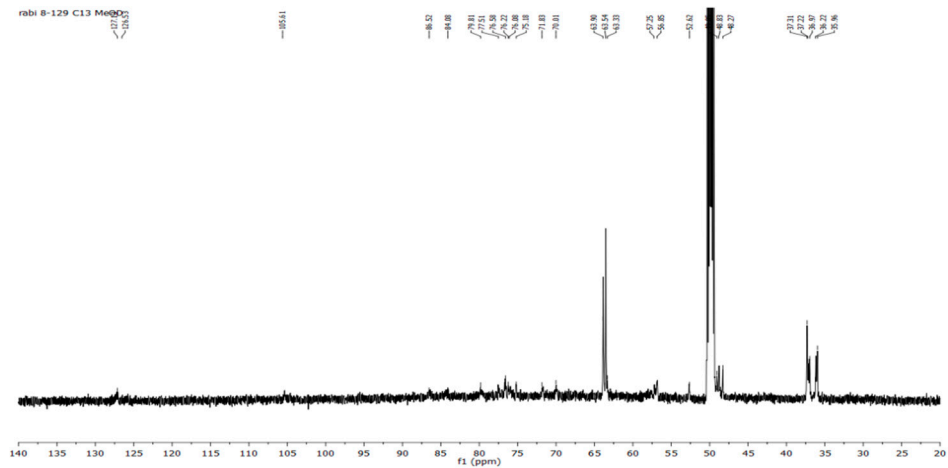


**Figure S41.**  $^{13}\text{C}$ -NMR spectrum of 17.

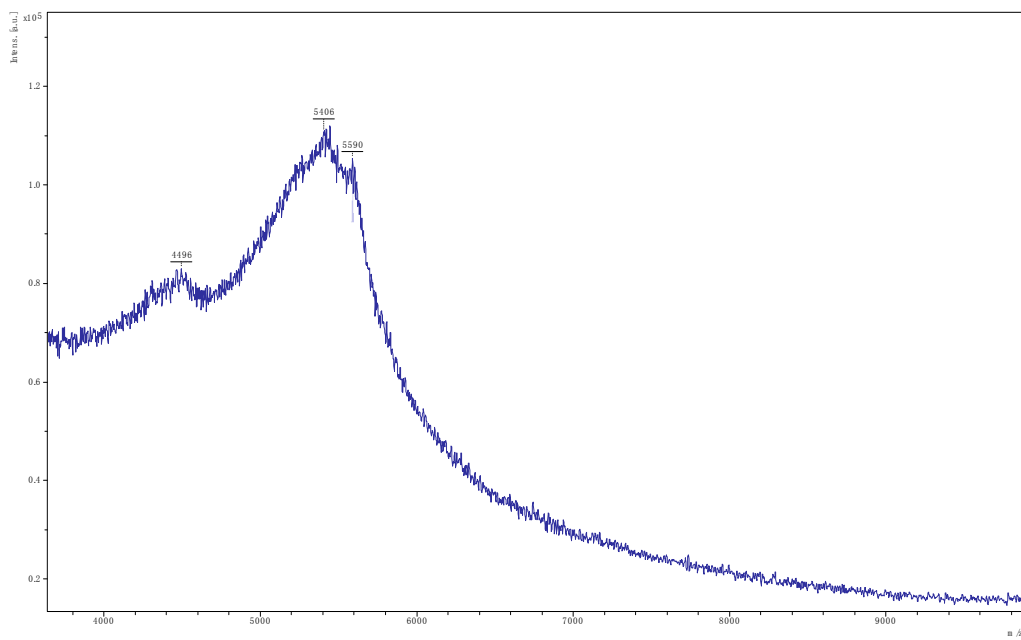


**Figure S42.** MALDI-tof of compound 17.

### 1.12. Dendrimer 18

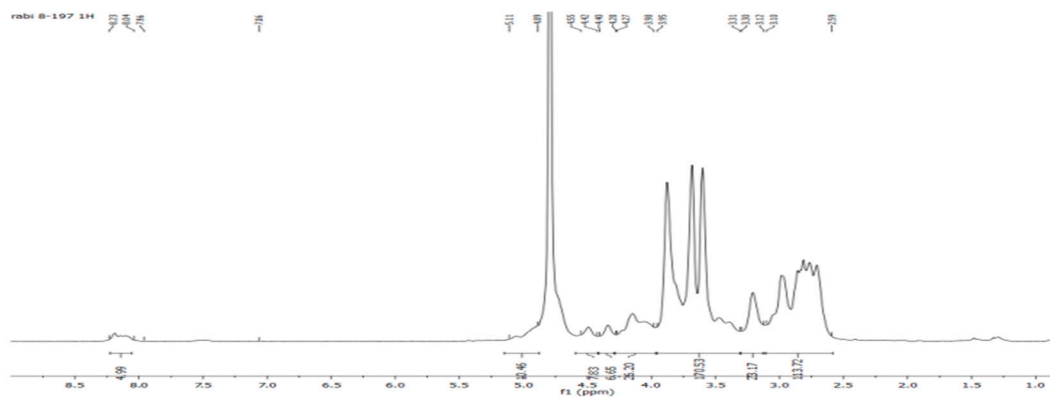
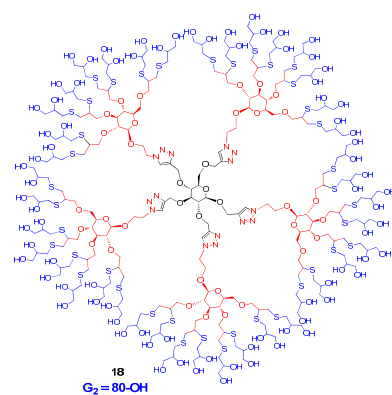


**Figure S43.**  $^1\text{H}$ -NMR ( $\text{D}_2\text{O}$ ) spectrum of **18**.

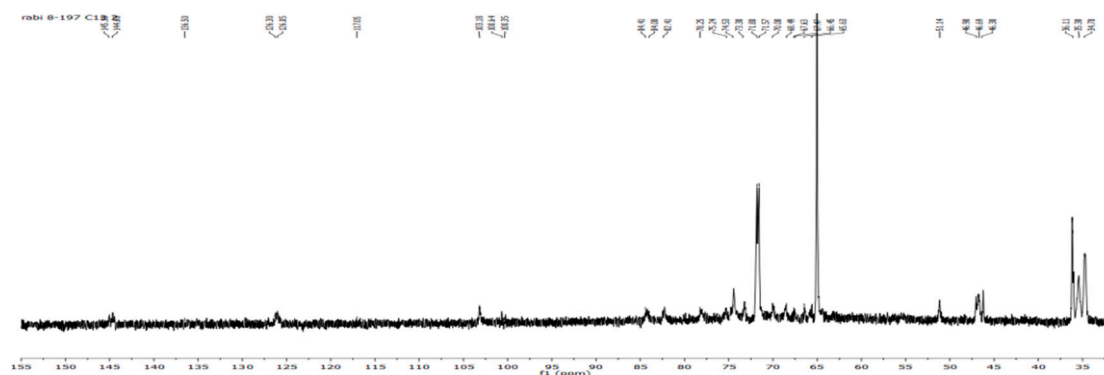


**Figure S44.**  $^{13}\text{C}$ -NMR spectrum of **18**.

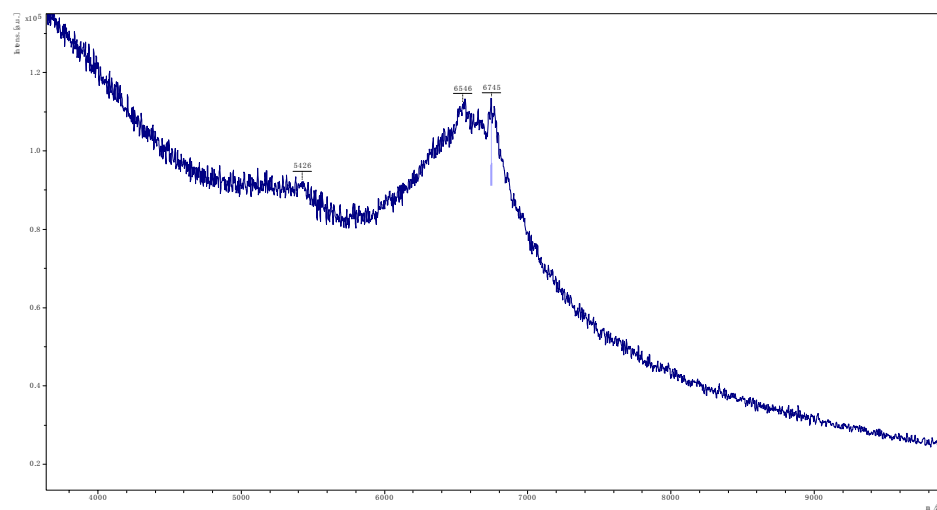


**Figure S45.** Maldi-tof of compound **18**.

### 1.13. Dendrimer 19

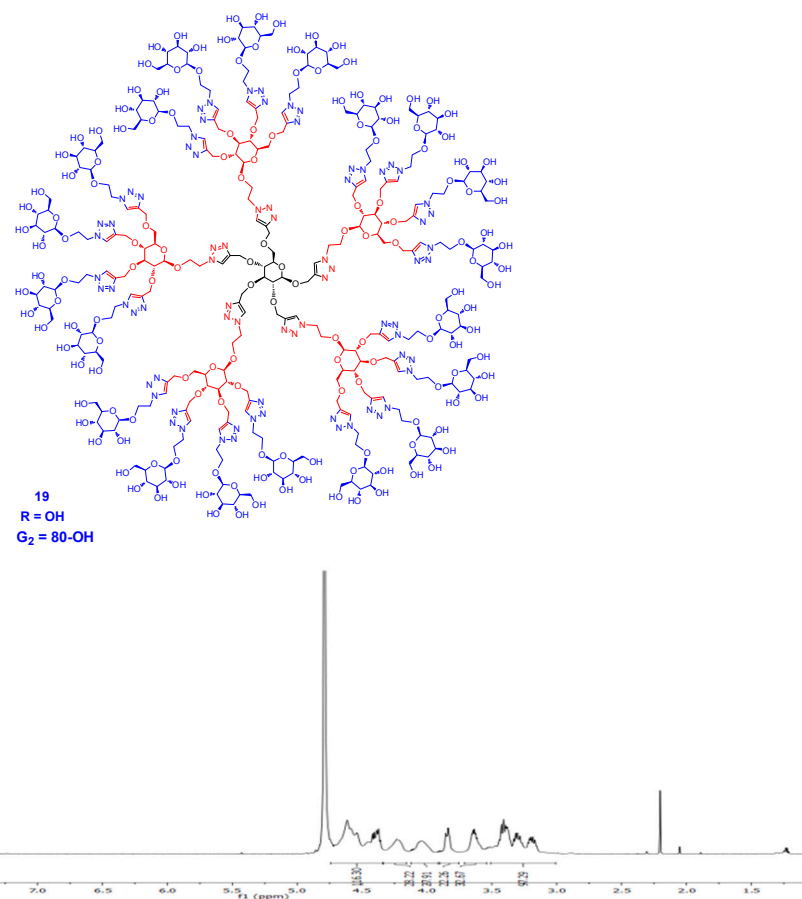


**Figure S46.**  $^1\text{H}$ -NMR ( $\text{D}_2\text{O}$ ) of **19**.

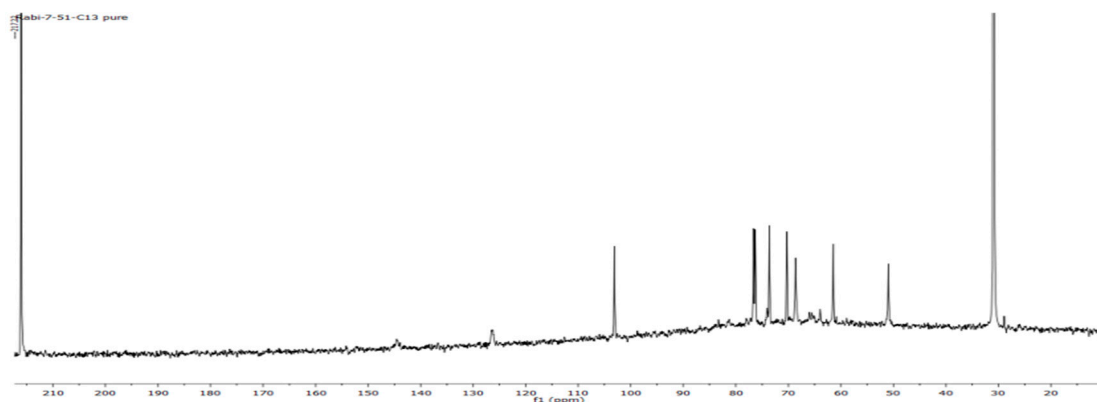


**Figure S47.** <sup>13</sup>C-NMR of **19**.

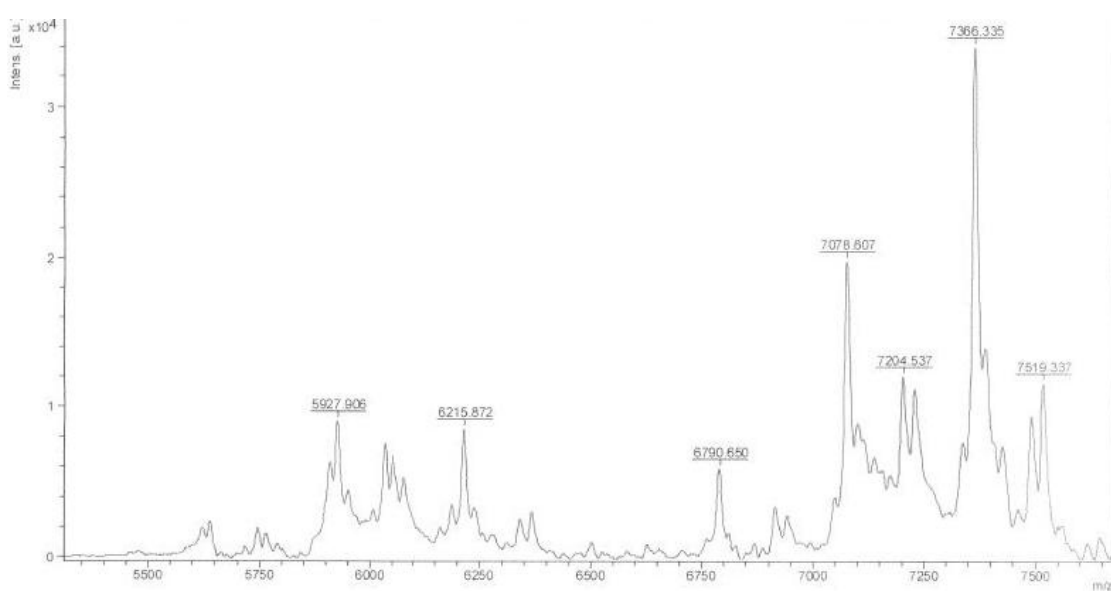


**Figure S48.** MALDI-TOF of Compound **19**.

### 1.14. Dendrimer 20

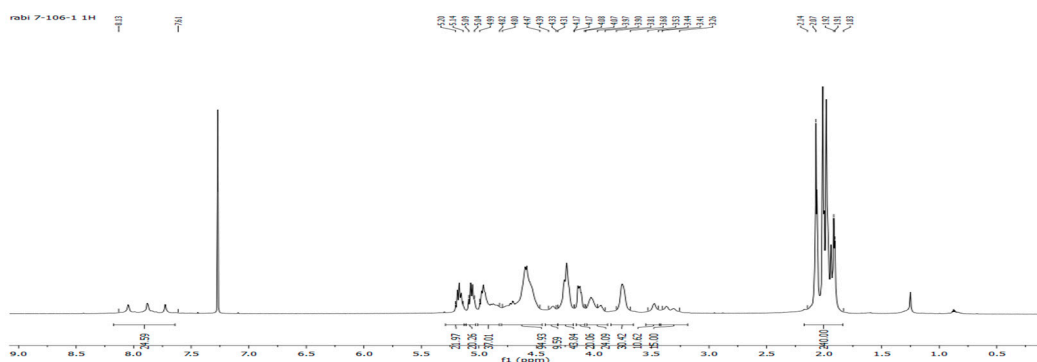
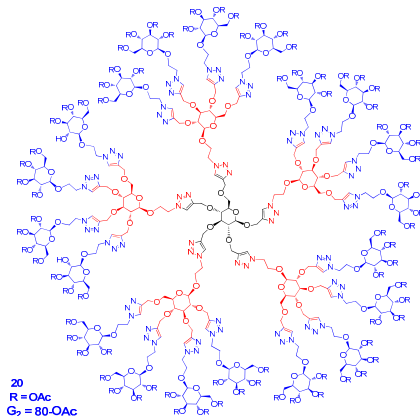


**Figure S49.**  $^1\text{H}$ -NMR ( $\text{CDCl}_3$ ) spectrum of **20**.

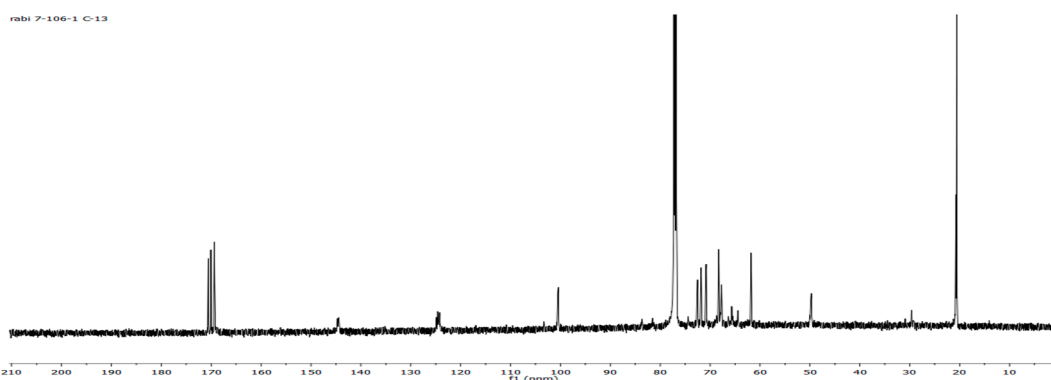


**Figure S50.**  $^{13}\text{C}$ -NMR spectrum of **20**.

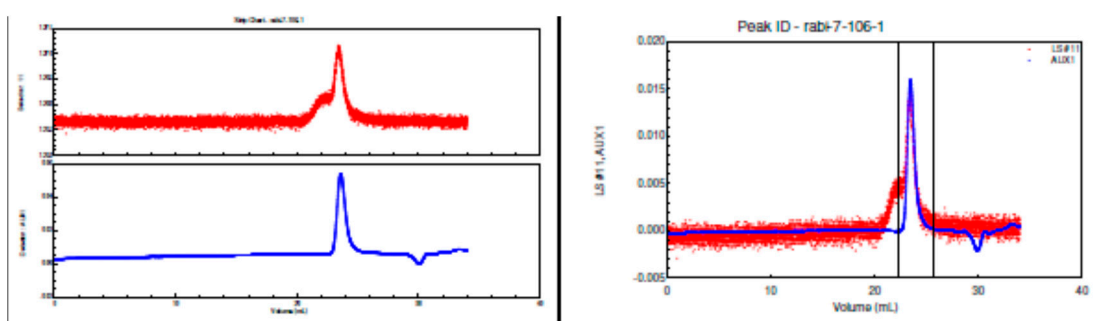


**Figure S51.** GPC of **20**.

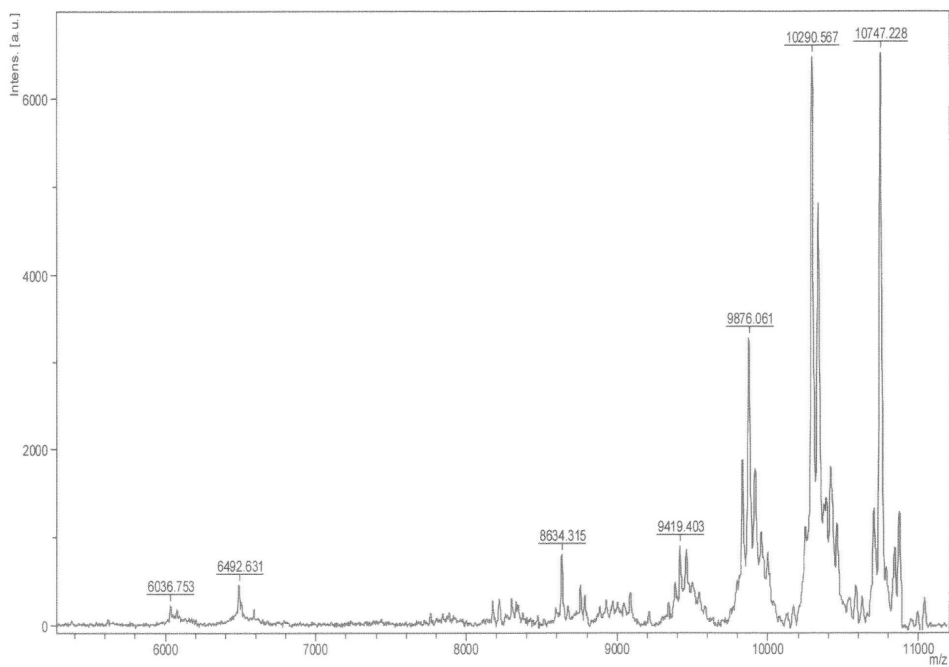
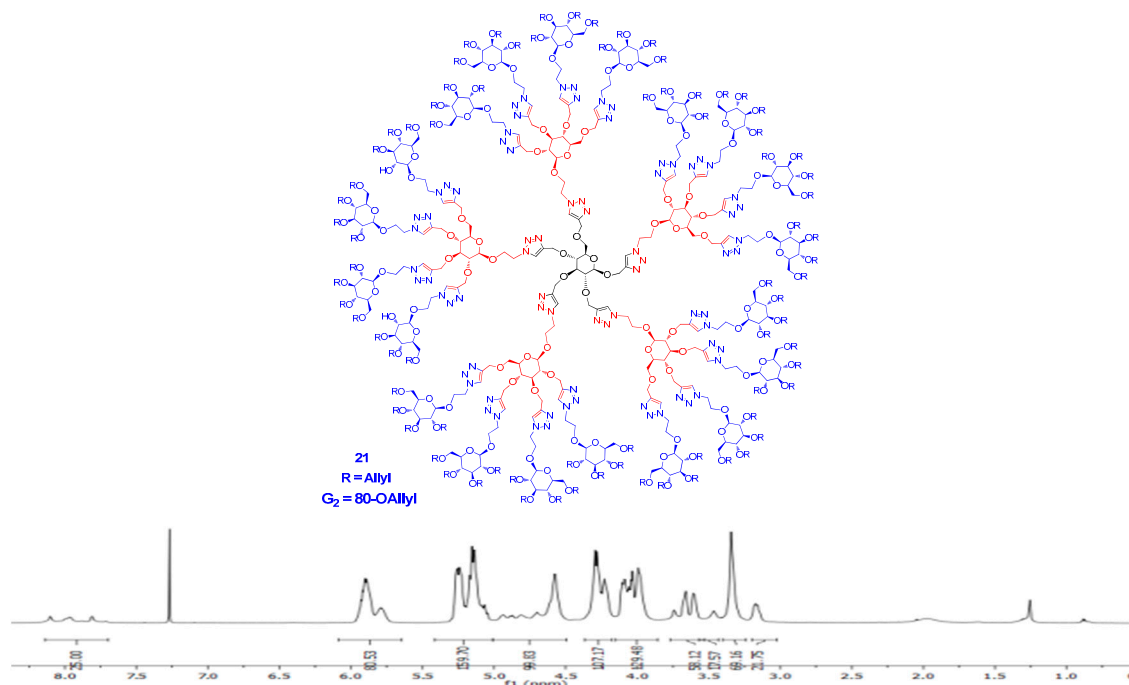
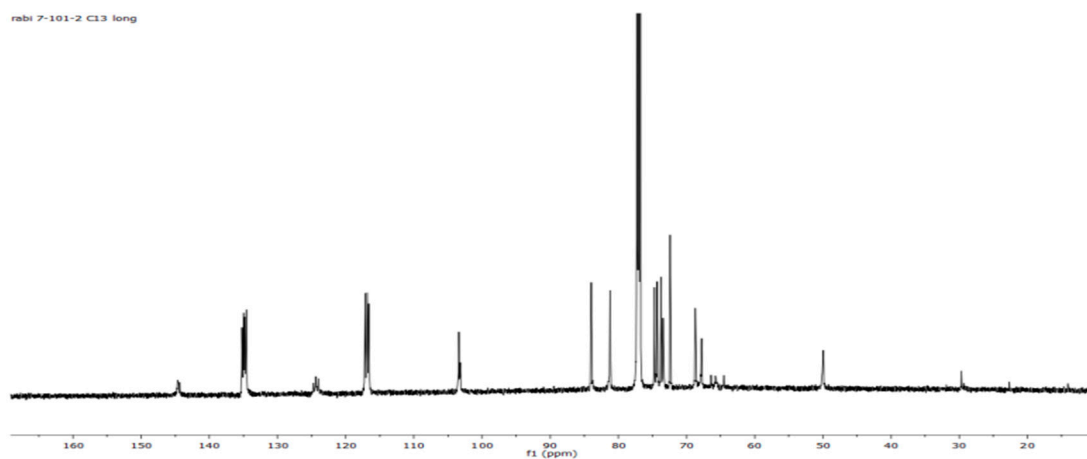


Figure S52. MALDI-TOF of Compound 20.

## 1.15. Dendrimer 21

Figure S53.  $^1\text{H}$ -NMR ( $\text{CDCl}_3$ ) spectrum of 21.



**Figure S54.** <sup>13</sup>C-NMR spectrum of **21**.

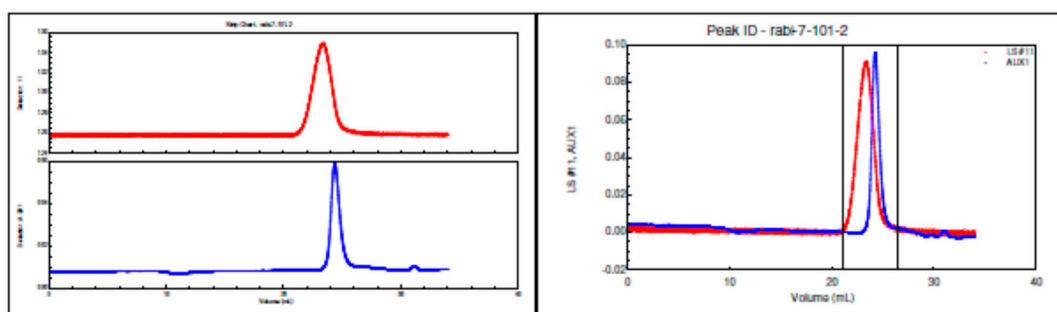


**Figure S55.** GPC of **21**.

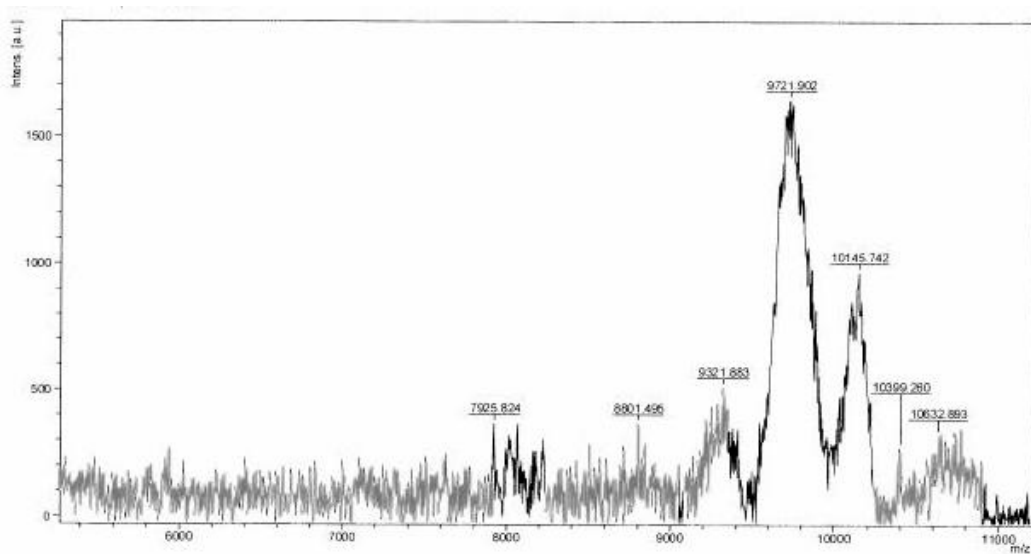


**Figure S56.** MALDI-TOF of Compound **21**.

## 2. Computational Methods

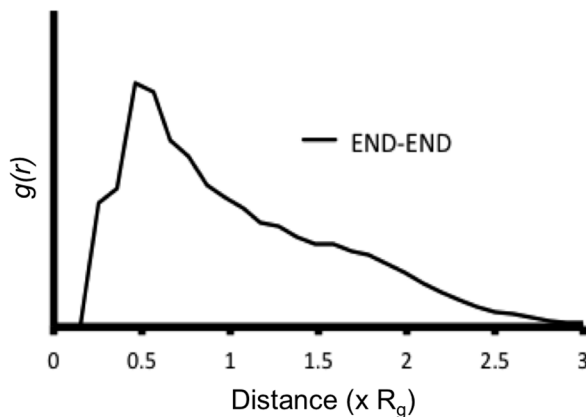


**Figure S57.** Radial distribution function ( $g(r)$ ) of the END groups as a function of the distance. The most probable distance between surface groups in equilibrated **16** is at *c.a.*  $0.5 \times R_g$  (i.e.,  $\approx 5 \text{ \AA}$ ).

**Table S1.** Main structural features of dendrimer **16** in solution at the equilibrium.

$R_g$ ( $\text{\AA}$ )	END-END avg. Distance <sup>[a]</sup> ( $\text{\AA}$ )	SASA ( $\text{\AA}^2$ )	$R_{\text{SASA}}^{[b]}$ ( $\text{\AA}$ )	$V_{\text{SASA}}^{[c]}$ ( $\text{\AA}^3$ )	$V_g^{[c]}$ ( $\text{\AA}^3$ )	$V_{\text{void}}^{[d]}$ ( $\text{\AA}^3$ )	Porosity <sup>[e]</sup>
9.8	5	3332	16.3	18124	4017	14107	0.78

<sup>[a]</sup> Calculated from the position of the END-END  $g(r)$  peak (Figure S57). <sup>[b]</sup> Calculated from SASA, being  $\text{SASA}=4\pi R_{\text{SASA}}^2$ . <sup>[c]</sup> Calculated as the volume of the spheres having radius  $R_g$  (“full” volume) or  $R_{\text{SASA}}$  (“total” volume). <sup>[d]</sup>  $V_{\text{void}}=V_{\text{SASA}}-V_g$ . <sup>[e]</sup> Dendrimer’s porosity is calculated as the ratio between void volume ( $V_{\text{void}}$ ) over the total one ( $V_{\text{SASA}}$ ).

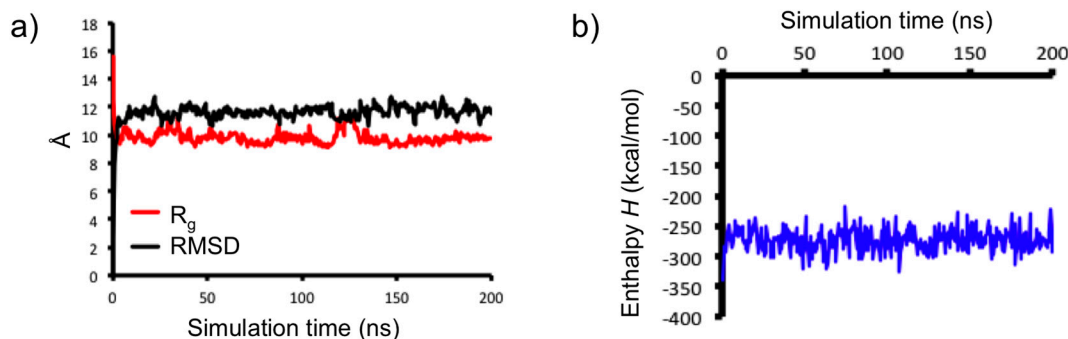


**Figure S58.** Equilibration of dendrimer **16** during the MD simulation. (a) Root mean square displacement (RMSD: black) and radius of gyration ( $R_g$ : red) data for **16** as a function of simulation time; (b) Enthalpy  $H$  of **16** calculated as the sum of solute-solute and solute-solvent interactions.